MINISTRY OF EDUCATION AND TRAINING
HCMC UNIVERSITY OF TECHNOLOGY AND EDUCATION

HO NGOC THE QUANG

RESEARCH ON ACTIVE VIBRATION REDUCTION METHODS USING FORCED EXTERNAL FORCES IN THE TURNING PROCESS

Major: Mechanical Engineering
Major Code: 9520103

PHD DISSERTATION SUMMARY

HO CHI MINH – 2024

This work was completed at HCMC University of Technology and Education

Scientific Supervisor 1: Assoc. Prof. Dr. Do Thanh Trung
Scientific Supervisor 2: Prof. Dr. Nguyen Xuan Hung

Opponent 1:
Opponent 2:
Opponent 3:

The dissertation will be defended before the University-Level Dissertation Evaluation Council at HCMC University of Technology and Education on …..

LIST OF PUBLISHED WORKS

1. The Ho, Q.N.; Do, T.T.; Son Minh, P. Studying the Factors Affecting Tool Vibration and Surface Quality during Turning through 3D Cutting Simulation and Machine Learning Model. Micromachines 2023, 14, 1025. https://doi.org/10.3390/mi14051025 (Q2)
2. The Ho, Q.N.; Do, T.T.; Minh, P.S.; Nguyen, V.-T.; Nguyen, V.T.T. Turning Chatter Detection Using a Multi-Input Convolutional Neural Network via Image and Sound Signal. Machines 2023, 11, 644. https://doi.org/10.3390/machines11060644 (SCIE - Q2)
3. Quang Ngoc The Ho, Thanh Trung Do. Effects of Workpiece Surface and Cutting Parameters on the Finished Surface Quality in Turning Based on Finite Element Method. Journal of Technical Education Science, [S. l.], n. 78B, p. 18–25, 2023. DOI: 10.54644/jte.78B.2023.1392.
4. Q. Ho, P. Minh, and T. Do, A Study on Machine Learning Application by Convolutional Neural Network Model Classifying Audio to Identify Vibration Phenomenon in the Turning Process. 2023. doi: 10.1109/ICSSE58758.2023.10227199.
5. Quang Ngoc The Ho, Pham Son Minh, Thanh Trung Do. "Effect of tool holder stiffness on the product surface roughness in turning process by using the simulation method", Proc. SPIE 12720, 2022 Workshop on Electronics Communication Engineering, 127200Q (28 June 2023); https://doi.org/10.1117/12.2675023.
6. Quang, H.N.T., Minh, P.S., Van Son, N., Khuyen, H.N., Thuan, B.T., Son, T.V.D. (2024). Study on the Damping Effect of Compliant Structure on the Milling Tool holder. In: Long, B.T., et al. Proceedings of the 3rd Annual International Conference on Material, Machines and Methods for Sustainable Development (MMMS2022). MMMS 2022. Lecture Notes in Mechanical Engineering. Springer, Cham. https://doi.org/10.1007/978-3-031-39090-6_18.
7. Pham Sơn Minh, Do Thanh Trung, Lam Thanh Binh, Ho Ngoc The Quang. Anh huong cua van toc cat den do nham be mat trong quy trinh tien ren bang can dao giam chan. Tap Chi Co Khi Viet Nam So 4 – 2016.
8. Nguyen Ngoc Phuong, Pham Son Minh, Nguyen Van Toan, Ho Ngoc The Quang. Anh huong cua can dao giam chan den do bong be mat cua qua trinh phay mat phang. Tap Chi Co Khi Viet Nam So 4 – 2016.
9. Pham Son Minh, Do Thanh Trung, Ho Ngoc The Quang, Phan The Nhan, Nguyen Thanh Giang, Bui The Phong. Anh huong cua do cung can dao tien đen chat luong be mat tien tru. Tap Chi Co Khi Viet Nam So 9 – 2016.

INTRODUCTION

1. Reasons for choosing the topic

Turning machining is one of the most common manufacturing methods, widely employed in the production of various types of products. The major issue currently is vibration during machining.

In all manufacturing plants and machining units today, there is always a demand for improving productivity and product quality. Manufacturers always aim to select cutting parameters: higher cutting speeds, greater cutting depths... to reduce manufacturing costs and gain competitive advantages. But the biggest obstacle nowadays is vibration during machining, and they cannot overcome this issue.

Therefore, the dissertation on ‘Research on active vibration reduction methods using forced external forces in the turning process ' is highly necessary. The research results of the dissertation serve as a scientific foundation and reference material for training and scientific research activities in engineering universities in general, particularly in the field of mechanical engineering, especially in mechanical machining. Furthermore, the research results also aim to transfer technology to entities in the field of mechanical product manufacturing through machining methods. The research results can be applied in companies with limited investment in expensive machinery as mentioned above to gain a competitive advantage. Especially, the research results will be beneficial for companies producing products with long, small-diameter shafts, thin-walled components, and components with small-diameter deep holes because these parts are prone to vibration.

2. Research objectives

Study the mechanical properties and factors influencing vibration phenomena during machining. From there, propose solutions to identify, detect, and mitigate or eliminate this vibration, specifically reducing vibration during hole machining using the method of using external forces from forced contact. The research aims to improve product quality during turning machining.

3. Research content

Study the overview and theoretical basis of issues related to metal cutting processes, vibration processes of machine technology systems, cutting tools, and workpieces. Establish simulation models, experimental models to investigate the characteristics of vibration phenomena, factors influencing vibration, as well as models for data collection, data processing to detect, mitigate, or eliminate vibration. Research methods for identifying and detecting vibration from collected data such as images, sounds, forces, and accelerations.

Study the influence of forces from magnetic fields on the vibration characteristics of cutting tools and the surface quality of machined parts with a magnetic field-assisted cutting model.

4. Research scope and limitations

The evaluation criterion assesses the vibration characteristics of the cutting tool through changes in cutting force and vibration acceleration along the main cutting direction.

- Hole turning model using Aluminum Alloy Al 6061 material
- Turning model of thin flange material SS400.

5. Research methodology

Simulation, machine learning methods, experimentation, data collection, and analysis to investigate the influence of magnetic forces on vibration characteristics and surface quality of finished components.

6. Scientific significance

Simulating the cutting process with various technological factors enables the investigation of elements impacting the time efficiency and cost-effectiveness compared to experimental trials.

Utilizing intelligent artificial intelligence tools to detect and decode the rules of complex nonlinear vibration phenomena mechanisms in machining.

Using altering the parameters of the mechanical system, external stiffening forces can modify the vibrational characteristics of the oscillatory system.

7. Practical value

From the research results, understanding the operating laws and the mechanisms of influence of parameters on vibration phenomena, through machine learning methods, can manufacture vibration detection devices and learn to predict the vibration laws of the system to understand the vibration characteristics of the existing system. With the results of studying the impact of magnetic force and successfully manufacturing a magnetic levitation system, a patent has been granted for a useful solution that can be applied in industries.

8. Structure of the thesis

Introduction, Chapter 1: Overview, Chapter 2: Theoretical Foundation, Chapter 3: Research Model Establishment, Chapter 4: Study of Factors Influencing Vibration Characteristics, Chapter 5: Machine Learning Application for Vibration Identification and Prediction, Chapter 6: Active Vibration Reduction Study Using External Forces, Conclusion and Recommendations

CHAPTER 1: OVERVIEW

1.1. Introduction to turning

Turning is the most common machining method, creating machined surfaces through two movements known as shaping movements: the rotational movement of the workpiece and the linear movement of the cutting tool.

1.2. Types of vibrations and instabilities in turning

1.2.1 Forced vibrations

These are vibrations that occur when an external dynamic excitation force acts on the structure of the technological system.

1.2.2 Natural vibrations

Natural vibrations of the technological system arise from impacts, such as when engaging a clutch or when the tool begins cutting.

1.2.3 Self-excited vibrations

Self-excited vibrations are vibrations that arise and persist during the cutting process. Self-excited vibrations are not caused by external excitation forces but rather by the inherent cutting process itself.

1.3. Research overview outside the country.

The research on vibrations during turning processes worldwide has garnered significant attention from both the research community and the machining industry. Vibrations during turning are a complex issue and can significantly affect machining quality and production efficiency. Therefore, many researchers and research organizations are investigating and developing methods and technologies to prevent or control vibrations during turning processes. Research on turning vibrations worldwide focuses on various aspects (Figure 1.1). Some studies concentrate on analyzing and understanding the mechanisms of vibration, including the effects of cutting parameters, tool geometry, material hardness, and other factors on vibration generation. Simulation and modeling methods are also employed to study and predict vibrations. Research also focuses on developing vibration monitoring tools and systems to track and detect vibrations. Technologies such as sound sensors, acceleration sensors, and automated monitoring systems are used to collect data and analyze signals to identify vibration occurrences. Additionally, studies explore vibration control methods to minimize the impact of vibrations on the turning process. These methods may include using automatic control systems, optimizing cutting parameters, improving tool designs, and utilizing special machining materials.

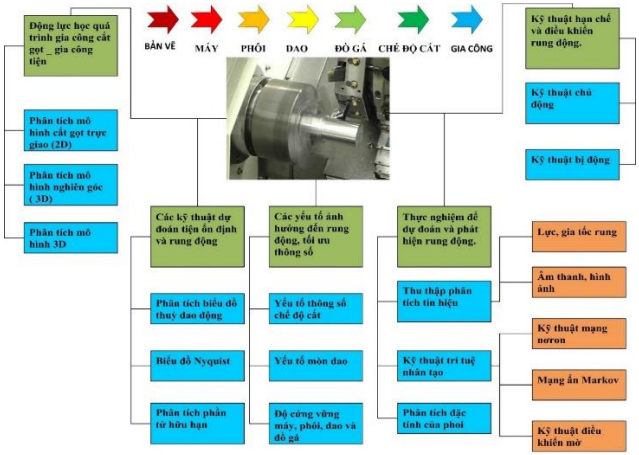

Figure 1.1: Research directions on vibrations in turning processes

1.3.1 Research directions on theoretical analysis and prediction of vibrations

1.3.2 Research directions on experimental prediction and identification of vibrations

1.3.3 Research directions on techniques and solutions for limiting and eliminating vibrations

1.4. Research overview within the country

In recent years, there have been numerous research works and projects on vibration processes in metal cutting. Notable works include "Self-excited vibrations and instabilities in metal cutting" by Assoc. Prof. Dr. Nguyen Dang Binh and Dr. Duong Phuc Ty. In this study, the authors synthesized all theoretical foundations and concepts in surveying vibration processes during metal cutting. Additionally, the authors proposed a new method for surveying vibration processes during metal cutting from an energy perspective.

Nguyen Thi Le Hang: Industrial University of Thai Nguyen - 2014: 'Assessment of the Positive Influence of Vibrations on Hard Turning'. The author presented a theoretical model of the positive influence of vibrations on the hard turning process and conducted experimental models to demonstrate it. The structure generating vibrations to assist the hard turning process based on the principle of ultrasonic vibrations (high frequency) was analyzed, designed, manufactured, and experimentally tested on 9XC steel.

1.5. Issues requiring further research

Through studies like the ones mentioned above, methods used to reduce oscillations focus solely on factors within the oscillation model during the

turning process: cutting conditions (self-generated forces), determining the parameters k, m, c, and the objects directly affecting the tooling technology system and the workpiece. With fixed parameters, these methods cannot be applied to models that vary in each production case.

The objective, through the method of applying external forces in addition to the existing forces on the oscillating system, is to limit the oscillation of the system. The project will focus on researching the following objectives:

$$m\ddot{x}(t) + c\dot{x}(t) + kx(t) = P(t) + P'(t) \qquad (1.1)$$

Developing mathematical models, simulating the process, and constructing experimental models of the impact process of external force P'(t) to reduce vibrations during turning.

CHAPTER 2 THEORETICAL FOUNDATIONS

2.1. Mechanics of metal cutting, vibrations phenomenon

The modeling of the single-degree-of-freedom turning tool vibration system is illustrated in Figure 2.1.

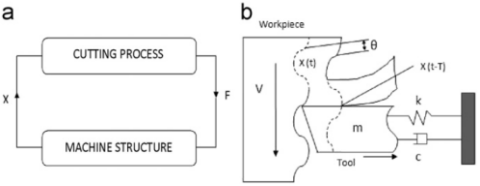

Figure 2.1: Interaction between the Tool and Cutting Process

And the characteristic equation of the single-degree-of-freedom vibration system is as follows:

$$m\ddot{x}(t) + c\dot{x}(t) + kx(t) = P(t) \qquad (2.1)$$

m: is the mass of the system.

c: damping coefficient of the system.

k: spring stiffness.

P(t) self-excited force due to metal cutting process along the x-axis with

$$P(t) = K_f b\left[x(t-T) - x(t)\right] \qquad (2.2)$$

K_f: cutting coefficient along the feed direction.

b: width of the workpiece layer (also cutting width) (mm)

T: time delay between the current time and the previous time.

$[x(t-T) - x(t)]$: variation in cutting thickness due to tool vibration..

2.2. Methods for evaluating machined surface quality

In this study, surface roughness parameters Ra and Rz are used as important criteria to evaluate vibration in both simulated and experimental turning

processes. When the system vibrates, surface roughness will be significant, resulting in low machined surface quality.

2.3. Finite element method (fem) simulation of turning processes

With the mathematical tool of Finite Element Method (FEM), it has been widely applied in solving differential equations in recent years. Software packages for machining simulation such as Third Wave AdvantEdge, Deform V11.0, and ABAQUS utilize the finite element method to simulate metal cutting processes as well as the analysis of cutting forces, making the method increasingly popular.

2.4. Taguchi theory

The Taguchi optimization method, also known as Taguchi Design and Improvement, is a technique used to optimize product quality and process performance. This method focuses on improving product quality or minimizing the influence of unanticipated factors on the process.

2.5. Neural network theory

2.5.1. Artificial neural network (ANN)

A neural network, also known as an Artificial Neural Network (ANN), is a computational system inspired by the workings of the human brain. It is a mathematical model consisting of a set of interconnected neuron nodes arranged in a defined structure. Each neuron node in the neural network receives input, performs a computation based on that input, and then passes the computed result to other neuron nodes in the network (Figure 2.2). The connections between neuron nodes contain weights, representing the strength of that connection. The computation process of the neural network is governed by these weights.

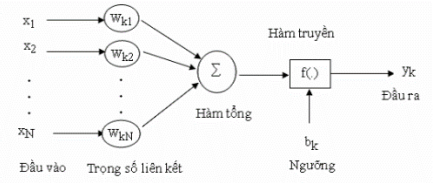

Figure 2.2: Basic Neural Network Diagram

2.5.2. Convolutional neural network (CNN)

Convolutional Neural Network (CNN) is a popular type of neural network for image classification tasks. Compared to traditional neural networks, CNN can integrate the spatial information of input data, enabling it to achieve better performance in image processing. The basic building block of a CNN is the convolutional layer, where training data is passed through filters to produce a set of activation maps corresponding to different features of the data (Figure 2.3).

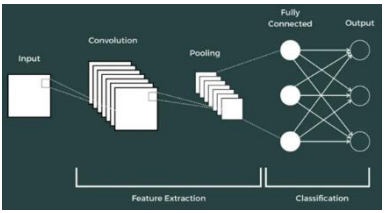

Figure 2.3: Basic Structure of CNN

2.6. Magnetic force calculation and mechanical-electromagnetic field simulation method

2.6.1. Calculating magnetic force using finite element method

2.6.2. Multiphysics mechanical-electromagnetic

The electromechanical problem is a technical term in the fields of electronics and mechanical engineering, combining both electrical and mechanical aspects to represent the interaction between electricity and mechanics in systems and devices (Figure 2.4). It involves the conversion and interaction between electrical and mechanical energy and typically refers to devices, technologies, or systems capable of converting between electrical and mechanical energy or utilizing both to operate. Electromechanical devices include electric motors, motor controllers, electrical and mechanical sensors, electric drive systems, and electronic and mechanical automation systems.

$$v_1 = i_1 R + \frac{\mu_0 A N^2}{2(l_0 - X_0)} \frac{di_1}{dt} + \frac{\mu_0 A N^2 I_0}{2(l_0 - X_0)^2} \frac{dx_1}{dt} \quad (2.3)$$

$$\frac{2\mu_0 A N^2 I_0 i_1}{4(l_0 - X_0)^2} = M \frac{dx_1}{dt^2} + B \frac{dx_1}{dt} + K x_1 + f_1 \quad (2.4)$$

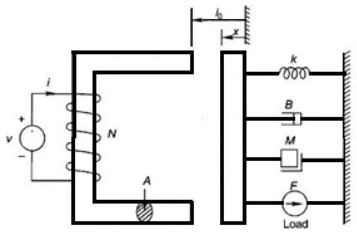

Figure 2.4: Diagram of Electromechanical Vibration Model

CHAPTER 3: SETTING UP THE RESEARCH MODEL

3.1. Turning process simulation model and magnetic force simulation

3.1.1. 2D turning simulation

The purpose of investigating the vibration process and its influence on surface roughness, the model is simplified to 2D with the tool and workpiece (Figure 3.1). In this model, the workpiece moves horizontally, while the tool remains stationary, and the boundary condition of the tool in the vertical direction is subject to stiffness k. The parameters of the workpiece, tool, and cutting conditions are presented in Table 3.1.

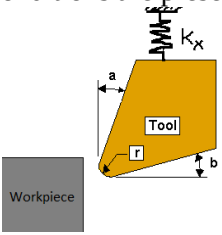

Figure 3.1: 2D Turning Model with Tool Stiffness Kx

Table 3.1: Parameters of Workpiece, Tool, and Cutting Conditions in 2D Simulation Model

Parameters		Value
Workpieces	Material	Al_6061
	Height	2 mm
	Long	5 mm
Tool	Rake angle	5^o
	Relief angle	10^o
	Cuttingedge radius	0.2 mm
	Material	Carbide
Cutting	Cutting Speed (v)	90- 290 m/min
	Feed (f)	0.1 - 0.5 mm/r
	Depth of cut	1 mm

3.1.2. 3D turning simulation

- Bar lathe simulation model

In this section, Author investigate the influence of the rigidity of the workpiece on the vibration and surface quality of the machined detail. Researcher simulate the lathe turning process using a longitudinal turning lathe model (Figure 3.2). The workpiece is fixed on a chuck, so the boundary conditions fix the end face of the workpiece for all motions (except the rotational motion of the workpiece). The tool model remains undeformed, with parameters listed in Table 3.2..

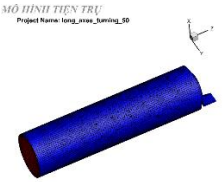

Figure 3.2: Bar Turning Model

Table 3.2: Parameters of the workpiece, tool, and cutting conditions in the 3D lathe turning simulation model

Parameter		Value
Workpiece	Material	Al_6061
	Diameter	4.5 - 10 mm
	Lenght	20 mm
Tool	Rake angle	5^o
	Relief angle	10^o
	Cuttingedge radius	0.2 mm
	Material	Carbide
Cutting	Spindle speed	2000 vòng/phút
	Feed (f)	0.15 mm/vòng
	Depth of cut	1 mm

- Simulation model of thin flange facing lathe

To study and evaluate the impact of the workpiece's rigidity on vibration and surface quality of the machined detail, a simulation model of the thin flange facing lathe process was utilized (Figure 3.3), with parameters outlined in Table 3.3.

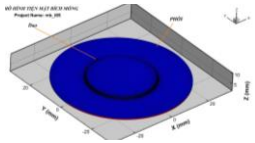

Figure 3.3: Thin Flange Facing Model

Table 3.3: Parameters of the workpiece, tool, and cutting conditions in the 3D thin flange facing lathe simulation model

Parameters		Value
Workpiece	Material	Al_6061
	Diameter	60 mm
	Cutting Diameter	40 mm
	Thickness	1.5 – 7 mm
Tool	Rake angle	5^o
	Relief angle	10^o
	Cuttingedge radius	0.2 mm
	Material	Carbide
Cutting	Spindle speed	2000 vòng/phút
	Feed (f)	0.15 mm/vòng
	Depth of cut	1 mm

- **Hole lathe simulation model**

In this section, the author simulates the machining process in a 3D model with a hole lathe model (Figure 3.4), considering both stable tool conditions and tool oscillation. From this, the time-dependent force values are extracted to evaluate tool stability through the dispersion of force values around the nominal force value. Additionally, the surface quality of the machined detail, represented by Rz, is extracted using simulation methods. The parameters of the hole lathe simulation model are shown in Table 3.4.

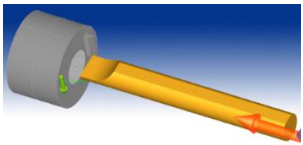

Figure 3.4:Drilling Lathe Model

Table 3.4: Parameters of the workpiece, tool, and cutting conditions in the hole lathe simulation model

Parameters		Value
Workpiece	Material	Al_6061
	Outer diameter/Hole Diameter	30 mm/12mm
	Lenght	30 mm
	Surface wave	0 – 0.2 mm
Tool	Rake angle	5^o
	Relief angle	10^o
	Cuttingedge radius	0.2 mm
	Material	Carbide
	Tool holder length	10–100 mm
Cutting	Spindle speed	40 – 125 m/phút
	Feed (f)	0.08–0.3 mm/vòng
	Depth of cut	1 mm

- **Magnetic force simulation model**

The model simulates the force generated by a direct current electromagnet. When a DC voltage is applied to the coil, the magnetic attraction force will pull the tool holder towards the magnet as shown in Figure 3.5.

During turning under the action of cutting force, the cutting tool tends to deform along the primary cutting direction. However, under the influence of the magnetic attraction force, it will tend to return to its balanced position, as shown in Figure 3.6.

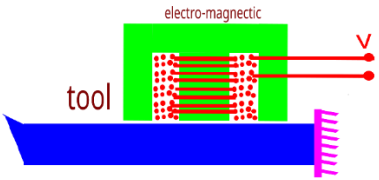

Figure 3.5: Turning Model under the Influence of Magnetic Force

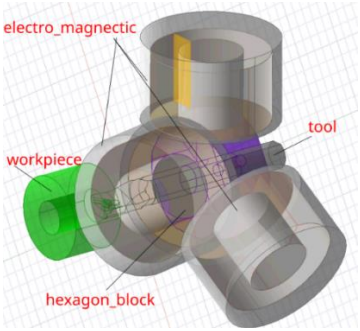

Figure 3.6: Tool holder model under the influence of 3 magnetic forces

3.2. Experimental model

3.2.1. Experimental model of thin flange facing turning (Figure 3.7)

Figure 3.7: sound collection during flange facing turning process

Table 3.5: Parameters of the workpiece, tool, and cutting conditions in the experimental model of thin flange facing

	Parameters	Value
Workpiece	Material	SS_400
	Diameter	220 mm
	Thickness	15 mm
Tool	Material	Carbide
	Rake angle	5°
	Relief angle	10°
	Cuttingedge radius	0.2 mm
	Tool holder length	50 mm
Cutting	Spindle speed	800 vòng/phút
	Feed (f)	0.1 mm/vòng
	Depth of cut	2 mm

3.2.2. Experimental model of active vibration reduction using external force

The experiment involved hole turning on aluminum Al T6061 material and was conducted using a Takisawa lathe machine (Figure 3.8). The parameters of the tool, tool holder, workpiece dimensions, and cutting conditions are presented in Table 3.6 :

Figure 3.8: Experimental Model of Magnetic Force

Table 3.6: Parameters of the tool, workpiece, and cutting conditions in the experimental model of magnetic force

	Parameters	Value
Workpiece	Material	AL6061
	Diameter	30 mm lỗ 12 mm
	Thickness	30 mm
Tool	Material	Carbide
	Rake angle	5°
	Relief angle	10°
	Cuttingedge radius	0.2 mm
	Tool holder length	80 mm
Cutting	Spindle speed	1020 vòng/phút
	Feed (f)	0.1 mm/vòng
	Depth of cut	0.2 mm

3.3. Neural network model

The machine learning model is presented with 4 input parameters and 2 output parameters, which are surface roughness Rz and cutting force oscillation amplitude Ra, as depicted in Figure 3.7.

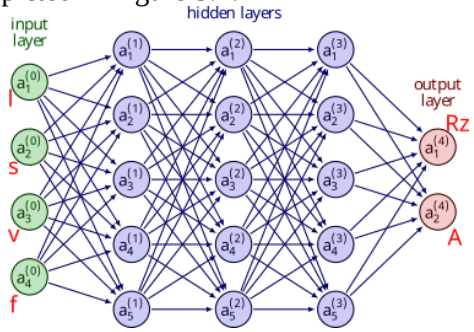

Figure 3.7: Neural Network Architecture

3.4. Vibration recognition model with two input data: sound and image

The study combined both input data factors, meaning that in a machining zone, two datasets were simultaneously collected: the image data of the machined surface and the corresponding sound data generated during cutting. The classification model is a CNN model with 2 input datasets.

CHAPTER 4: STUDYING FACTORS INFLUENCING VIBRATION CHARACTERISTICS

4.1. Influence of factors on machined surface quality using 2d simulation method

Figure 4.1: Signal-to-Noise Ratio (S/N) Chart

Figure 4.1 illustrates that the feed rate (f) has the greatest impact on the surface quality of the product. As the feed rate increases, surface roughness also increases, but the degree of influence varies at different stages. The feed rate particularly affects within the range from 0.1 - 0.2 mm and from 0.4 - 0.5 mm (steep slope). This can be explained by the fact that at a small feed rate, the material removal rate due to surface roughness of the workpiece is high, leading to significant variations in cutting load. On the other hand, at a feed rate of 0.5, the cutting force is higher, resulting in significant deformation of the tool holder. However, the least influence is observed within the range of f = 0.3 - 0.4. The surface wave of the workpiece is the second factor influencing surface quality. This indicates that the larger the surface wave on the product surface, the poorer the surface quality. However, the degree of influence is not clear due to the phase difference of the surface wave compared to the oscillation phase of the tool as presented above. Nonetheless, in this study, it was found that a wave step of s = 0.05 produces the best surface quality of the finished product.

4.2. Influence of workpiece stiffness on machined surface quality

4.2.1. Turning model

When analyzing the surface roughness of the product during longitudinal turning, it can be observed from Figure 4.2 that when the diameter of the workpiece ranges from 8 to 10 mm, the influence of deformation on surface roughness is not clearly visible. At that point, the surface roughness Rz remains stable within the range of 10 to 30 µm. This can be explained by the fact that when the workpiece diameter is rigid enough, its deformation is minimal. However, when the workpiece diameter is less than 7 mm, the variation increases rapidly, especially when the diameter is less than 5.5 mm. At this point, the

workpiece deformation becomes significant, leading to a sudden increase in surface roughness up to 225 µm. When the workpiece diameter is less than 4.5 mm, in this case, the turning process completely fails, and the actual turning process may fail, causing tool breakage or fracture.

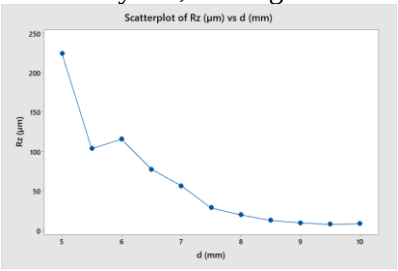

Figure 4.2: Relationship between surface roughness (Rz) and workpiece diameter (d)

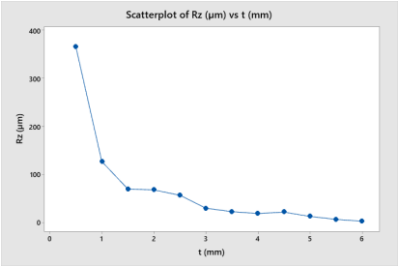

Figure 4.3: Relationship between surface roughness (Rz) and thin flange facing plate thickness (t)

4.2.2. Thin flange facing model

When analyzing the surface roughness of the product during thin flange facing, as shown in Figure 4.3, it can be observed that when the thickness of the facing plate is greater than 3 mm, the influence of workpiece surface deformation is not significant, and the surface roughness Rz remains stable within the range of 3 – 30 µm. This can be explained by the fact that when the thickness of the workpiece is sufficiently rigid, its deformation is minimal. However, when the thickness of the facing plate is less than 3 mm, the oscillation begins to increase rapidly, especially when the thickness of the facing plate is less than 1.5 mm. At this point, workpiece oscillation becomes significant, leading to a sudden increase in surface roughness up to 367 µm. In such cases, the actual turning process may fail, leading to tool breakage or fracture.

4.3. Simulation results and observations of the influence of factors on variation of force and surface quality of products in hole turning

4.3.1. Influence of tool holder length

The regression of the relationship between cutting force oscillation amplitude and surface roughness of the finished detail after machining depends on the length of the tool holder (Figure 4.4). For tool holder lengths less than 50-60 mm, we observe small surface roughness variations. This can be explained by the fact that with a short tool holder length up to an optimal value, the deformation of the tool holder is minimal. Consequently, the change in the relative position between the tool tip and the workpiece is insignificant, leading to minimal changes in cutting force. The tool achieves a stable state. This result

is of great significance for engineers to determine the optimal tool holder length to achieve stability.

During the tool holder length range from 60 mm to 85 mm, the surface roughness of the product increases rapidly. This is explained by the decrease in the stiffness of the tool holder, resulting in increased deformation and reduced relative position between the tool and the workpiece, leading to reduced cutting force. In this case, cutting and tool holder resilience forces are equivalent, resulting in significant tool oscillation. Conversely, when the tool holder is longer than 85 mm, the graph shows that the surface roughness of the workpiece tends to change less. This is because with a sufficiently long tool holder, although there is significant deformation, the tool holder resilience force is small, allowing the tool to establish a new position and oscillate around this new equilibrium position.

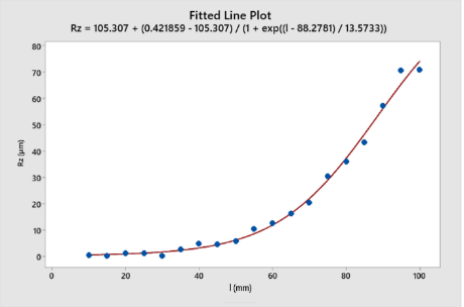

Figure 4.4: Regression analysis of the relationship between surface roughness and tool holder length

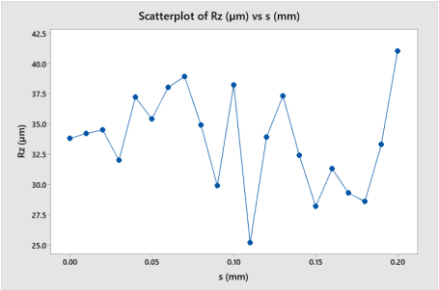

Figure 4.5: Relationship between product surface roughness and surface wave of the workpiece

4.3.2. Influence of surface wave of the workpiece

When the surface wave is large, the force amplitude changes. This is explained by the fact that a high surface wave amplitude leads to a larger cutting volume, resulting in a larger force amplitude variation. However, the force variation cycle remains almost unchanged. This is explained by the fact that the force variation cycle is mainly determined by the stiffness deformation of the tool holder, which is influenced by the length of the tool (Figure 4.5).

4.3.3. Influence of cutting speed

Figure 4.6 illustrates the simulation study results examining the relationship between cutting force variation and surface quality of the finished detail after

machining, with very little dependence on cutting speed. The variation values and trends are not clearly defined.

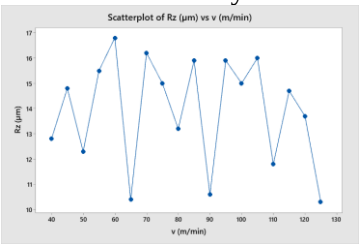

Figure 4.6: Relationship between product surface roughness and cutting speed

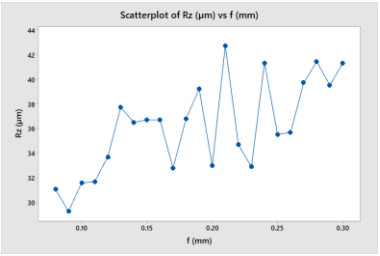

Figure 4.7: Relationship between product surface roughness and feed rate

4.3.4. The impact of feed rate

Figure 4.7 shows that with a feed rate ranging from 0.09 mm to 0.18 mm, the cutting force value significantly increases. However, the variation in cutting force over time is relatively small compared to the feed rate ranging from 0.21 mm to 0.30 mm. The results indicate that the amplitude of the cutting force change is greatest in the two cases of 0.21 mm and 0.30 mm. This can be explained by the fact that the vibration frequency of the tool holder is nearly equal to the undulation frequency of the workpiece at this feed rate, causing the system to enter a region of vibration.

4.3.5. Multi-factor impact

From the results in Table 4.8, it can be seen that the length of the tool holder has the greatest impact, as it determines the rigidity of the tool. The second most significant factor is the feed rate, followed by surface waviness and cutting speed, which rank third and fourth respectively. This is consistent with previous studies; however, this study additionally considers the factor of workpiece surface waviness, which was challenging to address in previous experimental studies.

Figure 4.8: Signal-to-Noise Ratio (S/N) 3D Model

4.4. Evaluation of the simulation results on the impact of various factors

The study investigated the impact of factors such as tool holder stiffness, cutting speed, feed rate, and workpiece surface waviness on the surface quality of the workpiece when turning, using finite element simulation on a 3D model. The study indicated that among the four factors, tool holder stiffness has the most significant impact. With a tool holder length of l = 60 mm in the simulation model, both the variation in cutting force and the surface quality of the finished workpiece, measured by Rz, reached optimal values.

CHAPTER 5: APPLICATION OF MACHINE LEARNING FOR VIBRATION RECOGNITION AND PREDICTION

5.1. Vibration recognition using sound

A total of 250 audio files were obtained, and based on the surface quality of the workpieces, they were evaluated as either stable or experiencing vibrations. Among the 250 workpieces, 200 were stable and 50 exhibited vibrations (Figure 5.1).

Figure 5.1: Experiment for collecting audio data of vibrating and stable workpieces during turning

The graphs below illustrate the accuracy and loss curves of the feature-extracted dataset using the VGG16 model. To extract features from the dataset, we employed transfer learning techniques and trained the models for 10 epochs.

The stability of the training process can be observed from epoch 4 onwards through the curves in Figure 5.2.

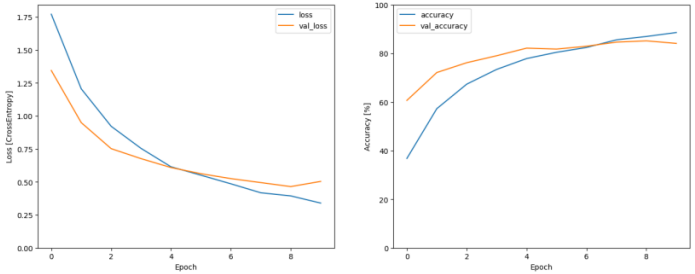

Figure 5.2: Accuracy on training and validation sets (left), loss value on training and validation data (right)

Among the 25 test data samples, 10 samples belong to the vibrating group during machining, and 15 samples belong to the stable group (Figure 5.3). After passing through the model, there are 8 samples in the vibrating group during machining and 17 samples in the stable group, indicating that the model made incorrect predictions on 2 samples. After evaluating the misclassified data, the model's predictive accuracy reached 92%. The model's accuracy is not high due to insufficient training data. To address the issue of data collection and improve model accuracy, the research will transition to a model for thin flange turning, which will provide more diverse and abundant data.

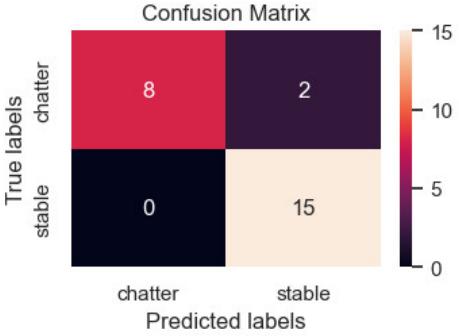

Figure 5.3: Confusion matrix of the model for vibration recognition using sound

5.2. Vibration recognition using sound and image

After identifying the stable and vibrating regions, the author used an electronic microscope to capture images of the surface detail of the finished workpieces in the marked areas. In regions labeled as vibrating and stable (Figure 5.4), a total of 1650 image files were obtained alongside 1650 audio files.

Subsequently, using a roughness measuring device to partition stable and vibrating regions, the author collected 987 image and audio files in the stable state and 663 image and audio files in the vibrating state.

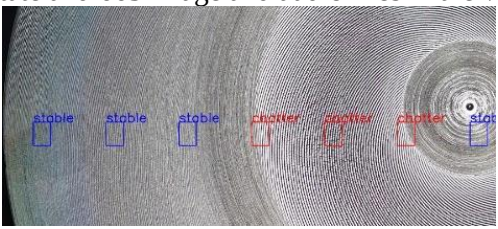

Figure 5.4: Product turning surface after roughness measurement and marking of stable and vibrating regions

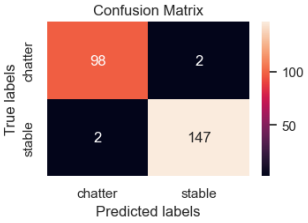

Figure 5.5: Confusion matrix of the dual input model

Among the 249 test data samples, there were 100 machining samples with vibrations, out of which the model incorrectly predicted 2 samples. Within the 149 images belonging to machining samples without vibrations, 3 data points were misclassified as vibrating, while the remaining 146 samples were classified correctly. After evaluating the misclassified data, the model achieved a predictive accuracy of 98%. As observed in Figure 5.5, the misclassified samples are distributed across both datasets.

Results of vibration recognition using CNN during machining (figures 5.6 and 5.7).

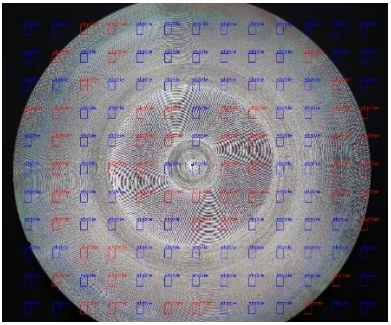

Figure 5.6: Applying the model for detecting vibrating surfaces

Figure 5.7: Vibration recognition during turning process

Table 5.1: Comparison of research results with recent studies

References	Methodology	Input data	Classification	Accuracy
This study	FFT	Images sounds	Binary	98 %
W. Zhu et al.	Size reduction	Images	Binary	98.26 %
Tran et al.	CWT	Images	Multilabel	99.67 %
Rahimi et al.	STFT	Images	Multilabel	98.90 %
Sener et al.	CWT	Images-cutting parameters	Multilabel	99.88 %
C. A. K. A. Kounta et al.	FFT	Sound_cutting	Multilabel	99.71%

5.3. Time-series force value prediction

With the time-series modeling approach, the predicted data closely matches the test data (Figure 5.8). This could be attributed to the experimental data being closely approximated by the model through machine learning algorithms, with discrepancies mainly due to noise factors and external influences.

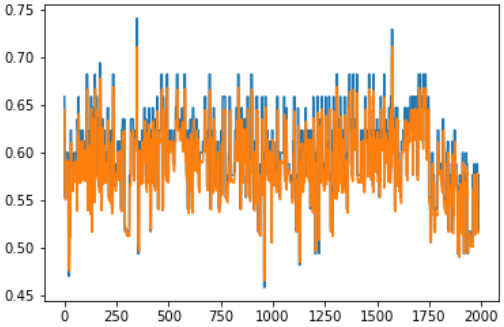

Figure 5.8: Comparison of predicted data and test data with LSTM model

CHAPTER 6: RESEARCH ON ACTIVE VIBRATION REDUCTION METHODS USING FORCED EXTERNAL FORCES

6.1. Simulation of tool holder deformation under the influence of magnetic force

The research results successfully simulated the magnetic force acting on the tool holder, depending on the distance between the tool holder and the magnet and the intensity of the current passing through the magnet (Figures 6.1 and 6.2).

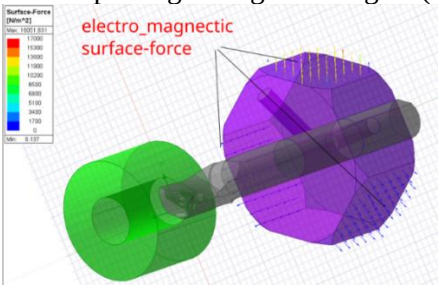

Figure 6.1: Magnetic force acting on the hexagonal block of the tool holder

Table 6.1: Displacement of the turning tool holder when applying magnetic force F_{1m}

STT	1	2	3	4	5	6	7	8	9	10
F_{1m} (N)	10	20	30	40	50	60	70	80	90	100
$\Delta_y(\mu m)$	3.3	6.2	9.4	12.6	15.5	18.7	22.1	24.8	30.6	31.6

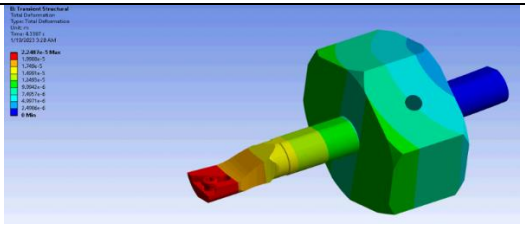

Figure 6.2: Tool holder displacement under the influence of magnetic force

6.2. Experimental results

After obtaining the characteristics of the magnetic force acting on the tool holder, the study concludes that it is possible to alter the oscillation characteristics of the tool holder under the influence of the magnetic force by varying the current intensity over time. The aim is to utilize the magnetic force

as an external force to reduce the fluctuation of cutting force and tool holder vibration. Experimental investigations assess the influence of the magnetic force from the magnetic holder on the vibration process and the surface quality of the machined products (Figure 6.3).

Figure 6.3: Experimental samples

6.2.1. Case of applying a force along the main cutting direction

The chart illustrating the relationship between surface roughness and imposed magnetic force is shown in Figure 6.4. On the chart, the x-axis represents the magnetic force, while the y-axis indicates the values of surface roughness Ra and Rz. Based on the graph, in the initial stage without magnetic force imposition, the corresponding surface roughness values are Ra = 3 μm and Rz = 15 μm. As the magnetic force gradually increases from 20 to 120 N, the surface roughness tends to decrease, indicating an improvement in surface quality. This can be explained by the fact that during the cutting process, the tool holder oscillates. However, as the magnetic force tends to pull the tool holder towards equilibrium, the tool holder vibrates less, and the oscillation cycle of the tool holder diminishes more rapidly. At F_{1m} = 140 N, the surface quality is optimal, with Ra = 1.7 μm and Rz = 9.1 μm. However, when increasing the magnetic force beyond F_{1m} > 140 N, the surface roughness tends to increase again. This could be explained by the fact that with higher magnetic force, the effect of the magnetic force cushion diminishes, and the magnetic force becomes greater than the cutting force, leading to increased tool holder oscillation.

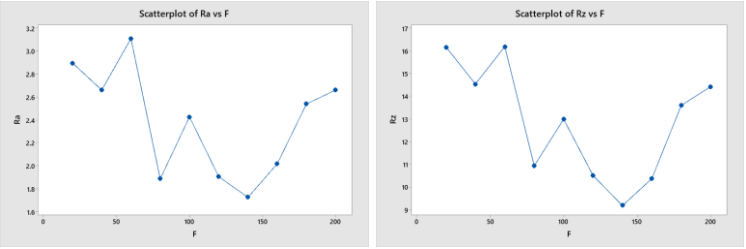

Figure 6.4: Relationship between magnetic force and surface roughness th1

6.2.2. Case of applying 2 forces along

6.2.2.1. Effects of 2 forces F_{1m} =2F_{2m}

The chart in Figure 6.5 illustrates the relationship between surface roughness and imposed magnetic force in the case of having 2 magnetic forces acting in 2 directions F_{1m} and F_{2m}, where F_{1m} = 2*F_{2m}. The x-axis of the chart represents the magnetic force, while the y-axis represents the surface roughness values measured by Ra and Rz. Based on the chart, we can observe that in the initial stage without magnetic force imposition, the surface roughness values corresponding to Ra are 4 μm and Rz is 20 μm..

As the magnetic force increases from 20 to 80, there is a tendency of surface roughness to decrease, indicating an improvement in surface quality. This can be explained by the gradual reduction in tool holder oscillation during cutting, as the magnetic force tends to pull the tool holder towards equilibrium, resulting in less vibration and a diminishing oscillation cycle of the tool holder. When the magnetic force reaches the level of F_{1m} = 100 N and F_{2m} = 50N, the surface quality peaks, with Ra values at 1.95 μm or Rz = 10.4 μm.

However, when the magnetic force increases beyond F_{1m} > 100 N and F_{2m} > 50N, the surface roughness tends to increase again. This could be explained by the diminishing effect of the magnetic force cushion and the magnetic force becoming greater than the cutting force, leading to increased oscillation of the cutting system.

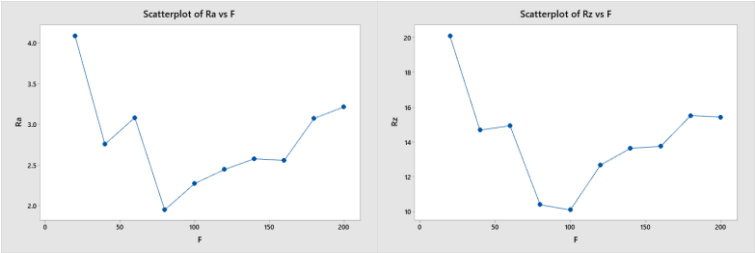

Figure 6.5: Relationship between magnetic force and surface roughness TH2

The optimal surface quality of the product is achieved at Ra = 1.95 μm; Rz = 10.4 μm corresponding to magnetic forces F_{1m} = 100 N and F_{2m} = 50N. It is 31% better than without magnetic force. When compared to case 1, the general trend remains, wherein increasing the imposed magnetic force enhances the surface quality of the finished product. However, when the magnetic force reaches the value of F_{mgh}, the vibration reduction effect of the magnetic force gradually diminishes, resulting in a decrease in surface quality.

6.2.2.2. Effects of 2 forces F_{1m} =F_{2m}

The chart in Figure 6.6 illustrates the relationship between surface roughness and imposed magnetic force in the scenario of having two magnetic forces acting along F_{1m} and F_{2m}, with F_{1m} = F_{2m}. The x-axis of the chart represents the magnetic force, while the y-axis represents the surface roughness values measured by Ra and Rz. Based on the chart, figure show that in the initial stage without magnetic force imposition, the surface roughness values corresponding to Ra are 3.7 μm and Rz is 17.4 μm.

As the magnetic force increases from 20 to 120 N, it is observed that the surface roughness tends to decrease, indicating an improvement in surface quality. This phenomenon can be explained by the reduced vibration of the cutting tool holder and the gradual decrease in cutting oscillation cycle during the cutting process, as the magnetic force tends to pull the tool holder towards equilibrium. When the magnetic force reaches the level of F_{1m} = 120 N and F_{2m} = 120N, the surface quality peaks with Ra values at 1.7 μm or Rz at 9.4 μm.

However, when the magnetic force increases beyond F_{1m} > 120 N and F_{2m} > 120N, the surface roughness tends to increase again. This phenomenon can be explained by the diminishing effect of the magnetic force and the magnetic force becoming greater than the cutting force, leading to increased vibration of the cutting system.

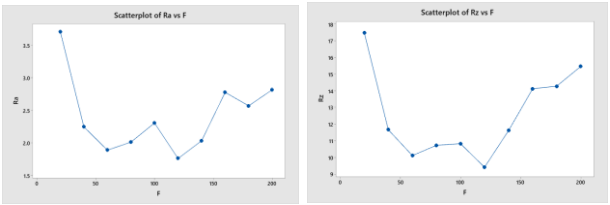

Figure 6.6: Relationship between magnetic force and surface roughness TH3

6.2.2.3. Effects of 2 forces F_{2m} =F_{3m}

The chart in Figure 6.7 shows the relationship between surface roughness and imposed magnetic force in the scenario of having two magnetic forces acting along F_{2m} and F_{3m}, with F_{2m} = F_{3m}. The x-axis of the chart represents the magnetic force ranging from 20N to 200N, while the y-axis represents the surface roughness values measured by Ra and Rz. Based on the chart, we can observe that in the initial stage without magnetic force imposition, the surface roughness values corresponding to Ra are 8.9 µm and Rz is 40.4 µm.

As the magnetic force increases from 20 to 60, it is observed that the surface roughness tends to decrease, indicating an improvement in surface quality. This phenomenon can be explained by the reduced vibration of the cutting tool holder and the gradual decrease in cutting oscillation cycle during the cutting process, as the magnetic force tends to pull the tool holder towards equilibrium. When the magnetic force reaches the level of F_{2m} = 60 N and F_{3m} = 60N, the surface quality peaks with Ra values at 1.6 µm or Rz at 8.8 µm.

However, when the magnetic force increases beyond F_{2m} > 60 N and F_{3m} > 60N, the surface roughness tends to increase again. This phenomenon can be explained by the diminishing effect of the magnetic force and the magnetic force becoming greater than the cutting force, leading to increased vibration of the cutting system.

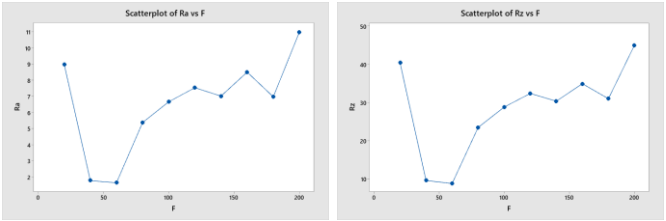

Figure 6.7: Relationship between magnetic force and surface roughness TH4

6.2.3. Effects of 3 forces in 3 directions

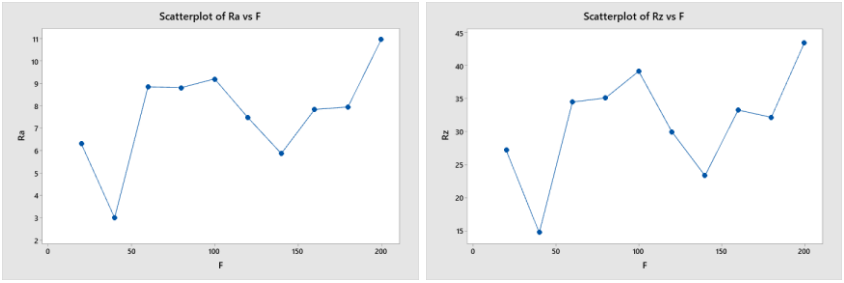

Figure 6.8: Relationship between magnetic force and surface roughness TH5

The surface quality of the detail is not better than the case without magnetic field.

6.3. Observations on the application of active vibration reduction method using external force

Figure 6.9: Vibrating machined products with magnetic field effect

The simulation results depicting the influence of the magnetic force on the behavior of the tool holder, the study successfully simulated a multi-physics environment including electromagnetic fields. By varying the current intensities passing through the coils as well as the distance from the magnet to the tool holder, the study simulated the forces acting on the tool holder and the deformation of the tool holder under the influence of the magnetic force (Figure 6.9).

The study conducted experiments with different magnetic force scenarios affecting the tool holder and measured the cutting force, acceleration, as well as the surface quality of the machined products. The study concluded that with the model of the magnetic forces F2m = F3m and a magnetic force value of 60N, the best surface quality of product can be achieved.

CONCLUSION AND RECOMMENDATIONS

1. Conclusion of the thesis

In the results of simulating the machining process in this thesis, it is evident that the cutting force varies over time, and this variation is highly sensitive to

changes in the input parameters of the simulation model. In the model, characteristic parameters such as cutting speed, cutting depth, and tool feed rate are assumed to be constant.

The study has proposed a new method for active vibration control, Magnetic Rest Active Control (MRAC), based on artificial neural network (ANN) which has been developed. .

2. Novelty of the thesis

Firstly, the thesis has employed numerical computation methods, specifically finite element method, to simulate the machining process.

Secondly, the thesis has successfully applied machine learning tools, a popular means nowadays, to detect vibration phenomena based on data collected during machining. Consequently, the vibration characteristics of the system during machining have been accurately identified.

Thirdly, the thesis has also succeeded in applying prediction algorithms in time series problems to forecast cutting force values.

Lastly, the thesis has also successfully designed and manufactured a Magnetic Rest Active Control (MRAC) system using DC electromagnets. The results of the cutting force prediction algorithm through machine learning can be applied to the magnetic force to improve vibration phenomena during machining. The development of this magnetic control system holds potential for reducing vibration in boring operations with long, slender tooling as well as when turning shafts with small diameter workpieces that lack rigidity.

3. Recommendations

In terms of simulation content, for further research on factors influencing vibration processes through simulation, subsequent studies should explore additional influencing models such as machining materials, tool wear, tool deflection...

The application of artificial intelligence to machining processes is a necessary and appealing field with significant potential. Neuron network models, in particular, are highly effective in addressing complex mechanical phenomena in cutting processes.